Polyhedron 103 (2016) 71–78

Contents lists available at ScienceDirect

Polyhedron

journal homepage: www.elsevier.com/locate/poly

Influence of Lewis acid charge and proximity in Mo≡Mo···M linear chain compounds with M = Na^+, Ca^{2+}, Sr^{2+}, and Y^{3+}

Brian S. Dolinar, John F. Berry *

Department of Chemistry, University of Wisconsin-Madison, 1101 University Avenue, Madison, WI 53706, United States

ARTICLE INFO

Article history:
Received 20 July 2015
Accepted 12 September 2015
Available online 16 September 2015

Keywords:
Dimolybdenum
Heterometallic
Alkali Metal
Alkaline Earth Metal
Quadruple bond

ABSTRACT

The syntheses, X-ray structural characterizations, and electrochemical properties of four new paddlewheel $[MMo_2(SNO5)_4Cl]^{(n-1)+}$ (M^{n+} = Na^+, Ca^{2+}, Sr^{2+}, Y^{3+}; HSNO5 = monothiosuccinimide) compounds are described here. By changing the M^{n+} cation charge and size, we demonstrate a method for easily tuning the Lewis acidity of the Mo≡Mo quadruple bond and the $[Mo_2]^{4+/5+}$ redox potential. As the charge of the M^{n+} cation is increased, the distal Mo atom becomes more Lewis acidic, leading to a shorter Mo_2–Cl bond distance, and the $[Mo_2]^{4+/5+}$ redox couple becomes less accessible. As the $M^{n+}\cdots Mo_2$ distance is increased, the distal Mo atom becomes less Lewis acidic, leading to a longer Mo_2–Cl bond distance.

1. Introduction

The chemistry of quadruply bonded $[Mo_2]^{4+}$ compounds has been studied for the past 50 years, and now it is a mature field [1]. Much of the current work in the field has focused on electronic and photophysical properties [2], reactivity [3], redox chemistry [4], and the use of Mo_2 units as building blocks in the synthesis of novel heterometallic compounds and supramolecular architectures [5]. The stability of the Mo≡Mo quadruple bond makes these compounds particularly robust and versatile.

Despite a wealth of chemistry based on equatorial ligand substitutions, Mo_2 complexes are not nearly as keen to bind ligands in the axial sites. For example, Mo_2 tetracarboxylates bind terminal chloride ions at distances ranging from 2.84 to 2.89 Å [6], significantly longer (by ⩾0.3 Å!) than the equatorial terminal Mo–Cl distances in the $[Mo_2Cl_8]^{2-}$ ion [7]. This attenuated axial Lewis acidity of Mo_2 complexes contrasts meaningfully with the strong Lewis acidity of the analogous Rh_2 compounds. The unparalleled catalytic behavior of Rh_2 compounds may be attributed to this Lewis acidity [8], which is instrumental in the stabilization of key intermediates in catalysis [8c, 9]. A major goal in the chemistry of metal–metal multiple bonds would be to endow complexes of the cheap, Earth abundant metal Mo with some of the chemical behavior more characteristic of Rh.

A topic of recent interest in coordination chemistry has been the effect of hard, redox-inactive, Lewis acidic main group metal ions on the chemical properties of transition metal complexes [10]. We hypothesized that a closely bound redox-inactive metal ion might increase the Lewis acidity of a quadruply-bonded Mo_2 unit. With this idea in mind, we designed the heterotrimetallic $[Mo_2]^{4+}$ compound pyLiMo_2(SNO5)$_4$Cl (**1**, SNO5 = monothiosuccinimidate, see Scheme 1), in which Lewis acidic Li^+ is held in the axial position of a $[Mo_2]^{4+}$ unit [5c]. The Li^+ ion serves to polarize the Mo≡Mo bond, increasing the Lewis acidity of the distal Mo atom and strengthening the Mo_2–Cl axial bond. The synthesis of **1** is facilitated by the ambidentate nature of the $SNO5^-$ ligand. The hard O donor atom preferentially binds to the hard acid Li^+ and the soft S donor atom preferentially binds to the soft acid Mo, allowing **1** to self-assemble from a mixture of $Mo_2(OAc)_4$, HSNO5, and LiCl (Scheme 1) [5c]. The ease with which **1** is synthesized suggests that the ambidentate nature of $SNO5^-$ can be harnessed to synthesize a variety of M···Mo_2 heterotrimetallic chain compounds.

Herein, we describe the syntheses, X-ray structural characterization, and electrochemistry of four new M···Mo_2 compounds (M = Na^+, Ca^{2+}, Sr^{2+}, Y^{3+}). The syntheses of these new compounds greatly expand the scope of M···Mo_2 heterotrimetallic compounds known, and we show that the $[Mo_2(SNO5)_4Cl]^-$ system can be generalized to interact with Lewis acids over a range of sizes and charges. Through the structural and electrochemical characterization of these compounds, the effect that cation charge and cation size have on the Lewis acidity and electronic properties of the $[Mo_2]^{4+}$ unit is probed.

* Corresponding author.
E-mail address: berry@chem.wisc.edu (J.F. Berry).

http://dx.doi.org/10.1016/j.poly.2015.09.028
0277-5387/

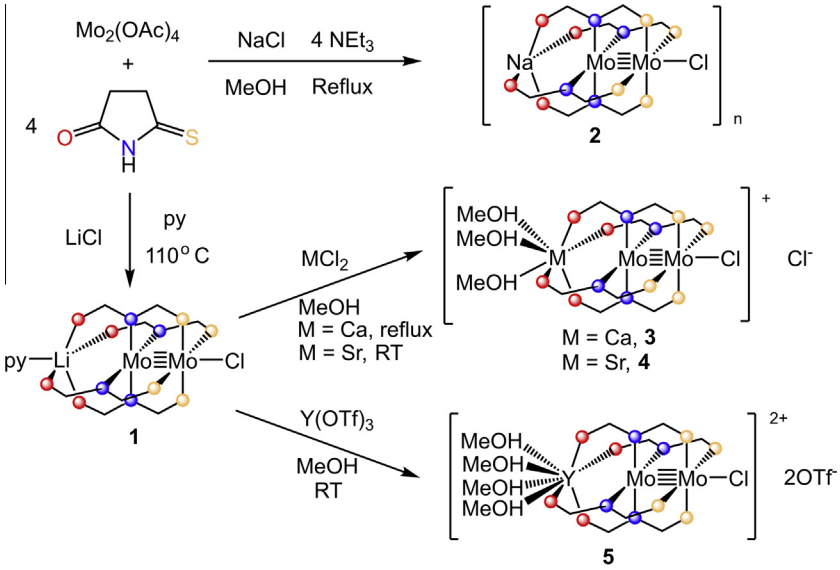

Scheme 1. Synthetic routes to compounds **1**–**5**.

2. Experimental

2.1. General

All synthetic work was carried out under an inert atmosphere using standard Schlenk and glovebox techniques. All solvents were rigorously dried prior to use. THF, MeCN, hexanes, and Et_2O were dried over molecular sieves and subsequently dried using a Vacuum Atmospheres solvent purification system and degassed prior to use. Pyridine was dried over molecular sieves, distilled from barium oxide under N_2, and stored in an inert atmosphere glovebox prior to use. MeOH was dried sequentially over molecular sieves and Mg/$Mg(OMe)_2$. It was then distilled under N_2 immediately prior to use. Propylene carbonate was purchased in anhydrous form from Sigma Aldrich and further dried by refluxing over CaH_2 for 72 h. It was then distilled under N_2 and stored in a glovebox prior to use. Monothiosuccinimide (HSNO5) was synthesized from succinimide and P_4S_{10} [11]. Molybdenum acetate ($Mo_2(OAc)_4$) was synthesized from $Mo(CO)_6$, acetic acid, and acetic anhydride [12]. **1**·py was synthesized from $Mo_2(OAc)_4$, HSNO5, and LiCl [5c]. All other reagents were purchased from Sigma–Aldrich and used without further purification. Elemental analyses were carried out by Midwest Microlabs in Indianapolis, IN, USA. NMR spectroscopy was performed on a Bruker AC 300 MHz spectrometer or Bruker Avance III 500 MHz Spectrometer. FTIR (ATR) data were obtained using a Bruker TENSOR 27 spectrometer.

2.2. Syntheses

2.2.1. Sodiumdimolybdenum-chlorotetrakis(monothiosuccinimidato) ($NaMo_2(SNO5)_4Cl$) (**2**)

A 100 mL Schlenk flask was charged with 138 mg HSNO5 (1.20 mmol), 440 mg NaCl (7.5 mmol), and 60 mL MeOH. To the resulting suspension was added 190 μL NEt_3 (1.36 mmol), and the mixture was stirred at 60 °C until the NaCl had fully dissolved. This solution was then transferred *via* cannula to a flask containing 127 mg $Mo_2(OAc)_4$ (0.297 mmol). The reaction mixture became an orange color, and there was a slow precipitation of orange-brown solid over a period of 5 min. The reaction mixture was heated at 70 °C overnight. Then, the reaction mixture was cooled to room temperature, filtered, and the solid was washed with 2 × 25 mL MeOH and 2 × 25 mL DCM. The remaining solid was extracted with 15 mL pyridine and layered with hexanes, yielding small crystals of **2**. The crystals were collected, washed with 3 × 30 mL hexanes, and dried under vacuum. Yield: 56 mg (27%). *Anal.* Calc. for $C_{18.5}H_{18.5}N_{4.5}O_4S_4Mo_2NaCl$ (**2**·0.5 C_5H_5N): C, 29.77; H, 2.50; N, 8.44. Found: C, 29.81; H, 2.64; N, 7.81%. ^{1}H NMR (500 MHz, DMSO-d6) δ 3.53 (br, 8H, S=CCH_2CH$_2$C=O), 2.77 (m, 8H, S=CCH$_2$-CH_2C=O). IR (ATR, cm^{-1}) 1728 (s), 1437 (m), 1457 (m), 1396 (s), 1240 (w), 1193 (vs), 1115 (w), 1050 (w), 911 (m), 806 (m), 667 (s).

2.2.2. Tris-methanol-calciumdimolybdenumchloro-tetrakis(monothiosuccinimidato) chloride [$(MeOH)_3CaMo_2(SNO5)_4Cl][Cl]$ (**3**)

A 50 mL flask was charged with 164 mg **1**·py (0.193 mmol), 700 mg $CaCl_2$ (6.31 mmol), and 20 mL MeOH. The reaction mixture was heated with stirring at 70 °C for 5 h. The mixture was filtered, and the filtrate was collected. After standing overnight, crystals of (**3**) formed. These crystals were filtered and washed with 2 × 10 mL MeOH. The solid was then dried under vacuum and collected. Yield: 65 mg (39%). *Anal.* Calc. for $C_{19}H_{28}N_4S_4O_7Mo_2$-$CaCl_2$: C, 26.67; H, 3.30; N, 6.55. Found: C, 27.16; H, 2.60; N, 7.12%. ^{1}H NMR (300 MHz, DMSO-d^6) δ 3.49 (m, 8H, S=CCH_2CH$_2$-C=O), 3.15 (s, CH_3OH), 2.73 (m, 8H, S=CCH$_2$CH_2C=O) ppm. IR (ATR, cm^{-1}) 1723 (vs) 1654 (vw), 1388 (m) 1270 (vs), 1248 (vs) 1230 (vs) 1026 (w), 679 (w).

2.2.3. Tris-methanol-strontiumdimolybdenumchloro-tetrakis (monothiosuccinimidato) chloride [$(MeOH)_3SrMo_2(SNO5)_4Cl][Cl]$ (**4**)

Analogously to the synthesis of **3**, A 100 mL Schlenk flask was charged with 173 mg **1**·py (0.204 mmol) and 1.9 g $SrCl_2$ (12 mmol). These were dissolved in MeOH at room temperature and stirred overnight resulting in the production of an orange precipitate. The solid was collected by filtration and washed with 2 × 25 mL Et_2O. Yield: 46 mg (25%). X-ray quality crystals could be obtained from concentration of the red–orange filtrate to 5 mL. ^{1}H NMR (DMSO-d^6) δ 3.51 (m, 8H, S=CCH_2CH$_2$C=O), 3.17 (s, CH_3OH), 3.15 (s, CH_3OH), 2.74 (m, 8H, S=CCH$_2$CH_2C=O), IR(ATR, cm^{-1}) 1716 (s), 1611 (vw), 1429 (w), 1385 (m), 1260 (vs), 1238 (vs), 1222 (vs), 1101 (m, br), 804 (w), 681 (m).

2.2.4. Tetrakis-methanol-yttriumdimolybdenum-chloro-tetrakis-monothiosuccinimidato bis-triflate [$(MeOH)_4YMo_2(SNO5)_4Cl][OTf]_2$ (5)

A flask was charged with 1.32 g $Y(OTf)_3$ (2.46 mmol) and 199 mg **1**·py (0.234 mmol). These were dissolved in 10 mL of MeOH. The reaction mixture was stirred at room temperature

overnight. Then the reaction mixture was filtered and layered with 80 mL Et_2O. Within a week, X-ray quality crystals of (**5**) grew. The crystals were collected by filtration, washed with 3 x 50 mL Et_2O, and dried under vacuum. Yield: 140 mg (50%). *Anal.* Calc. for $C_{22.15}H_{32}N_4S_{6.15}O_{14.45}F_{6.45}YMo_2Cl_{0.85}$ (0.85·**5** + 0.15·[$(MeOH)_4YMo_2(SNO5)_4$][$OTf]_3$), C, 21.88; H, 2.65; N, 4.61. Found: C, 21.43; H, 2.65; N, 4.45%. ^{1}H NMR (500 MHz, DMSO-d6) δ 3.49 (m, 8H, S=CCH_2CH_2C=O), 3.17 (s, CH_3OH), 3.15 (s, CH_3OH), 2.74 (m, 8H, S=CCH$_2$CH_2C=O). IR (ATR, cm^{-1}) 1696 (m), 1657 (w), 1405 (m), 1394 (m), 1382 (m), 1290 (s), 1258 (vs), 1225 (s), 1166 (w), 1066 (s), 1028 (vs), 880 (w), 802 (w), 761 (vw), 698 (m), 637 (s).

2.3. X-ray crystallography

Single crystals of **2**·4py, **3**·2MeOH, **3-dim**·5.5 MeCN, **4**·2MeOH and **5**·1.6MeOH were selected under paratone oil and attached to a MiTeGen MicroMount. They were mounted in a stream of cold N_2 at 100(1) K using an Oxford Cryostat and centered in the X-ray beam using a video monitoring system. The crystal evaluation and data collection were performed on a Bruker Quazar APEX-II diffractometer with Mo Kα radiation (λ = 0.71073 Å). The data were collected using a routine to survey an entire sphere of reciprocal space. The data were integrated using the SAINT routine in APEX-II and corrected for absorption using SADABS [13]. The structures were solved *via* direct methods and refined by iterative cycles of least-squares refinement on F^2 followed by difference Fourier synthesis using SHELX2013 [14] (see Table 1). All non-hydrogen atoms were refined anisotropically except where noted below. The alcohol hydrogen atoms on MeOH components of structures **3**·2MeOH, **4**·2MeOH, and **5**·1.6MeOH were located from the Fourier difference map and refined independently. All other hydrogen atoms were included in the final structure factor calculation at idealized positions and were allowed to ride on the neighboring atoms with relative isotropic displacement coefficients. The positional and compositional disorder present in these structures is detailed in the Supporting Information.

2.4. Electrochemistry

Compounds **1**, **2**, **3**, and **5** were dissolved in propylene carbonate and chloride was removed by addition of a slight excess of $TlPF_6$, giving dehalogenated compounds **1a**, **2a**, **3a**, and **5a**. The gray TlCl that precipitated was removed by filtration. Cyclic voltammograms for compounds **1a**, **2a**, **3a**, and **5a** were taken in propylene carbonate at room temperature with 2 mM analyte and 100 mM electrolyte (NEt_4PF_6) using a standard glassy carbon electrode for the working electrode, a platinum wire for the auxiliary electrode, and an Ag/Ag$^+$ electrode as the reference electrode. The solutions were titrated with the appropriate M$(OTf)_n$ until the redox wave no longer changed. All electrochemical potentials were internally referenced to the ferrocene/ferrocenium couple. The voltammetry was performed in the range of 1000 mV to 0 mV at a scan rate of 100 mV s^{-1}.

3. Results and discussion

3.1. Synthesis

Each compound reported here was synthesized by one of two methods: self-assembly or cation exchange of Li$^+$ for M^{n+}. Compound **2** was synthesized by the self-assembly method shown in Scheme 1. In this method, the acetate ligands of $Mo_2(OAc)_4$ are substituted for HSNO5 while simultaneously installing the Na$^+$ ion into the compound. In this reaction, the Na$^+$ is first allowed to bind to the deprotonated SNO5$^-$ ligand in MeOH at 60° C. Then, the Na$^+$-ligand solution is added to $Mo_2(OAc)_4$ and heated to reflux to give the desired compound. Without NaCl in the reaction, *cis*-2,2-$Mo_2(SNO5)_4$ is predominantly produced [2b]. Indeed, this reaction also generates some *cis*-2,2-$Mo_2(SNO5)_4$ as a byproduct, but allowing Na$^+$ and HSNO5 to precomplex before adding the $Mo_2(OAc)_4$ limits the amount of this undesired byproduct that is formed. The presence of Na$^+$ thus appears to template the desired 4,0 arrangement of the ligands, similar to the role of Li$^+$ in the synthesis of **1** [5c].

In solution, the Li$^+$ ion of **1** only has a modest thermodynamic preference for binding (K_{eq} = 95 at 298 K) [5c]. Thus, **1** is potentially a good starting material for the preparation of a variety of M···Mo_2 compounds by cation exchange. Compounds **3**–**5** were synthesized in this manner, by exchanging Li$^+$ for either Ca^{2+}, Sr^{2+}, or Y^{3+} (Scheme 1). In these reactions, either $CaCl_2$, $SrCl_2$, or Y$(OTf)_3$ is reacted with **1** in MeOH. Compound **1** is only sparingly soluble in MeOH, but when the incoming metal is present in solution, **1** easily dissolves and reacts to form the desired compound as a precipitate. These reactions can be either done at reflux (compound **3**) or room temperature (compounds **4** and **5**). While the former does yield a successful synthesis of the compound, it also forms a significant amount of *cis*-2,2-$Mo_2(SNO5)_4$ that must be removed, and reactions at room temperature avoid this complication.

3.2. X-ray crystal structures

The X-ray crystal structures of **2**–**5** are shown in Figs. 1–4, and important bond distances of **2**–**5** are compiled in Table 2 and compared with those of **1**·py and its dimer [$LiMo_2(SNO5)_4Cl]_2$ (**1-dim**). Each compound has a very similar Mo≡Mo bond distance between 2.12 Å and 2.14 Å. These distances are longer than the average Mo≡Mo bond distance of $[Mo_2]^{4+}$ paddlewheel compounds found in the CSD (~2.10 Å), likely due to electron donation into σ^* and π^* orbitals of the Mo_2 unit by the axial ligands [5c,15]. Compounds **2**–**5** each exhibit the same 4,0 arrangement of SNO5 ligands found in **1**·py and **1-dim**. The differences between these structures lie in the coordination environment, charge, and ionic radius of their Lewis acidic main group cations.

Structure **2**·4py is polymeric, with the Na$^+$ ion coordinated to a bridging chloride of an adjacent molecule as well as the four SNO5$^-$ ligands, giving a square pyramidal coordination geometry around the Na$^+$ ion. The Na···Mo_2 distance is 3.505(2) Å, which is substantially longer than the Li···Mo_2 distances found in **1**·py and **1-dim** (3.075(5) Å and 3.049(6) Å, respectively). The Mo_2–Cl bond distance increases from 2.6533(6) Å in **1**·py to 2.776(1) Å in **2**·4py. Since Na$^+$ is more remote from the $[Mo_2]^{4+}$ core than Li$^+$ is, it has less of an influence on the acidity of the $[Mo_2]^{4+}$. The lower Lewis acidity as well as the bridging nature of the axial Cl$^-$ contribute to the increased Mo_2–Cl bond distance in this compound as compared to the Li complex.

The Ca^{2+} and Sr^{2+} ions of **3**·2MeOH and **4**·2MeOH are coordinated by three MeOH ligands as well as the four SNO5 ligands, giving a seven-coordinate mono-capped trigonal prismatic geometry with one SNO5$^-$ O atom in the capping position. These structures also contain two solvent MeOH molecules. One of these forms a hydrogen bond with the free Cl$^-$, and one of these forms a hydrogen bond with the axially bound Cl$^-$, which serves to lengthen the Mo_2–Cl bond. The complexes have M···Mo_2 distances of 3.699(1) Å and 3.8138(5) Å, respectively, which are significantly larger than that of **2**·4py. For **4**·2MeOH, this is expected, since Sr^{2+} has a much larger ionic radius than Na$^+$, but for **3**·2MeOH, this is unexpected. The ionic radii of 5-coordinate Na$^+$ and 7-coordinate Ca^{2+} are 1.14 Å and 1.20 Å, respectively. However, the average M–O_{SNO5} bond distance is essentially identical for the two compounds,

Table 1
X-ray experimental data for structures **2–5.**

Compound	**2**·4py	**3**·2MeOH	**3-dim**·5.5CH_3CN	**4**·2MeOH	**5**·1.6MeOH
Formula	$C_{16}H_{16}ClMo_2N_4NaO_4S_4$·4 ($C_5H_5N$)	$[C_{19}H_{28}N_4O_7S_4ClCaMo_2]Cl$·2 ($CH_3OH$)	$C_{32}H_{32}Ca_2Cl_4Mo_4N_8O_8S_8$·5.5 ($CH_3CN$)	$[C_{19}H_{28}Cl_2Mo_2N_4O_7S_4Sr]Cl$·2 ($CH_3OH$)	$C_{20}H_{32}Cl_{0.85}Mo_2N_4O_8S_4Y[CF_3SO_3]_{2.15}$·1.6 ($CH_3OH$)
Formula weight	1023.29	919.64	1773.08	967.18	1260.11
T (K)	100.0	100.0	100.0	100.01	100.0
Crystal system	tetragonal	orthorhombic	orthorhombic	orthorhombic	monoclinic
Space group	*P4/ncc*	*Pbca*	*Pnma*	*Pbca*	$P2_1/c$
a (Å)	13.402(4)	19.139(7)	26.379(9)	19.1231(9)	12.156(4)
b (Å)	13.402(4)	14.502(5)	16.334(6)	14.5719(7)	14.561(5)
c (Å)	22.289(6)	24.573(8)	15.656(6)	24.850(1)	25.45(1)
α (°)	90	90	90	90	90
β (°)	90	90	90	90	102.61(1)
γ (°)	90	90	90	90	90
V (Å^3)	4003(3)	6821(4)	6746(4)	6924.7(6)	4396(3)
Z	4	8	4	8	4
ρ_{calc} mg/mm^3	1.698	1.791	1.746	1.855	1.904
μ (mm^{-1})	0.964	1.338	1.342	2.694	2.308
F(000)	2064.0	3712.0	3534.0	3856.0	2509.0
Crystal size (mm)	0.476 × 0.232 × 0.078	0.04 × 0.03 × 0.03	0.098 × 0.065 × 0.063	0.164 × 0.025 × 0.023	0.247 × 0.086 × 0.080
Radiation	Mo Kα (λ = 0.71073)	Mo Kα (λ = 0.71073)	Mo Kα (λ = 0.71073)	Mo Kα (λ = 0.71073)	Mo Kα (λ = 0.71073)
2θ range for data collection	3.654 to 64.276°	3.314 to 55.23	3.024 to 54.798	3.278 to 52.804	3.242 to 52.878
Independent reflections	3527	7917	7924	7089	8995
R_{int}	0.0314	0.0786	0.0848	0.1088	0.0547
Data/restraints/parameters	3527/168/185	7917/38/433	7924/930/566	7089/39/430	8995/192/632
Goodness-of-fit (GOF) on F^2	1.121	1.061	1.134	1.021	1.418
Final R indexes [$I \geqslant 2\sigma(I)$] [a,b]	R_1 = 0.0257	R_1 = 0.0243	R_1 = 0.0415	R_1 = 0.0346	R_1 = 0.0699
	wR_2 = 0.0709	wR_2 = 0.0482	wR_2 = 0.0945	wR_2 = 0.0625	wR_2 = 0.1430
Final R indexes [all data]	R_1 = 0.0287	R_1 = 0.0387	R_1 = 0.0568	R_1 = 0.0608	R_1 = 0.0808
	wR_2 = 0.0744	wR_2 = 0.0531	wR_2 = 0.1010	wR_2 = 0.0699	wR_2 = 0.1460

[a] $R_1 = [\Sigma||F_o| - |F_c||]/[\Sigma|F_o|]$.
[b] $wR_2 = [\Sigma[w(F_o^2 - F_c^2)^2]]/[\Sigma(w(F_o^2)^2]]^{1/2}$, $w = 1/[\sigma^2(F_o^2) + (aP)^2 + bP]$, where $P = [\max(0 \text{ or } F_o^2) + 2(F_c^2)]/3$.

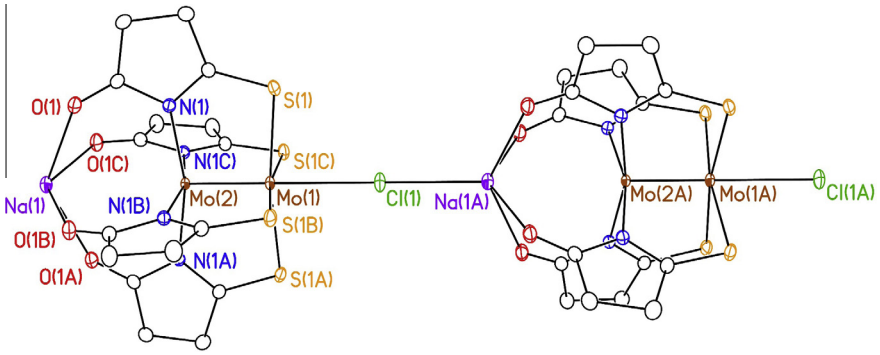

Fig. 1. X-ray crystal structure of polymeric **2**·4py. Atoms are drawn as 50% thermal probability ellipsoids. All hydrogen atoms and solvent molecules are omitted for clarity.

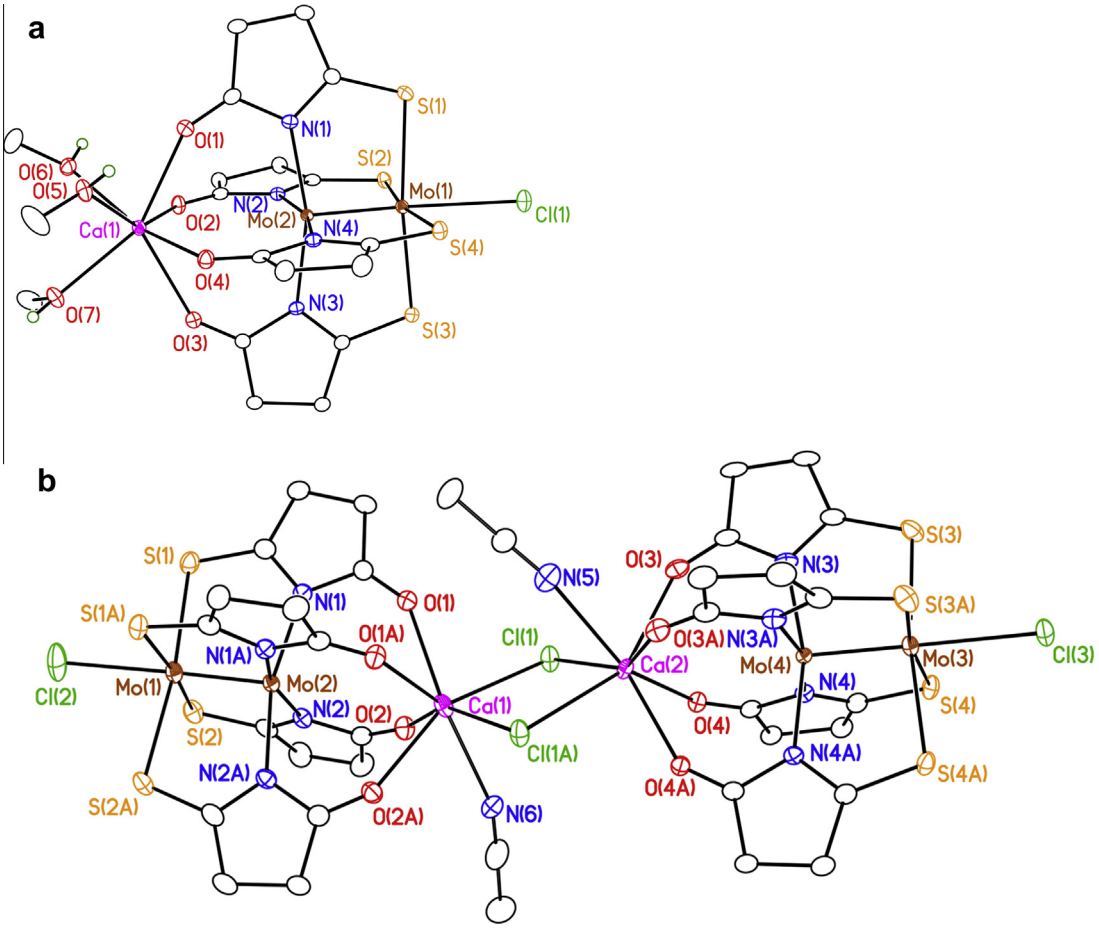

Fig. 2. X-ray crystal structures of (a) monomeric **3** and (b) dimeric **3-dim**. All atoms are drawn as 50% thermal probability ellipsoids. All hydrogen atoms, except the alcohol hydrogens of methanol, all counter ions, minor components of disorder, and free solvent molecules are omitted for clarity.

indicating that the difference in ionic radii between Na^+ and Ca^{2+} has a negligible impact on the structure and does not adequately explain the ~0.19 Å increase in M···Mo_2 separation. Instead, we believe this change to result from Coulombic repulsion between $[Mo_2]^{4+}$ and M^{n+}. The Mo^{2+} ions of the dimolybdenum unit more strongly repel the Ca^{2+} ion than the Na^+ ion because of the higher charge on Ca^{2+}, resulting in the longer M···Mo_2 separation. In spite of the longer M···Mo_2 distance as well as the hydrogen bonding interaction between solvent MeOH and the axial Cl^-, both **3**·2MeOH and **4**·2MeOH have Mo_2–Cl bond distances (2.7023(9) Å and 2.707(1) Å, respectively) that are significantly shorter than the Mo_2–Cl bond distance in **2**·4py. While the increased charge of Ca^{2+} is responsible for the increased M···Mo_2 distance, the increased charge also exerts a greater influence on $[Mo_2]^{4+}$, resulting in a Mo_2–Cl bond distance closer to that in the corresponding Li^+ compound. The Mo_2–Cl bond distance of **4**·2MeOH is slightly longer than that of **3**·2MeOH. This slight increase is likely caused by the slightly longer M···Mo_2 distance of the Sr^{2+} compound.

When crystallized from MeCN, **3** dimerizes to form the structure **3-dim**·5.5 MeCN. In this structure, both Ca^{2+} ions are coordinated by four SNO5 ligands, two chlorides, which bridge the two halves of the dimer, and one MeCN ligand. This structure has a slightly longer M···Mo distance than does **3**·2MeOH, but it has a much shorter Mo_2–Cl bond distance of 2.630[1] Å. This Mo_2–Cl

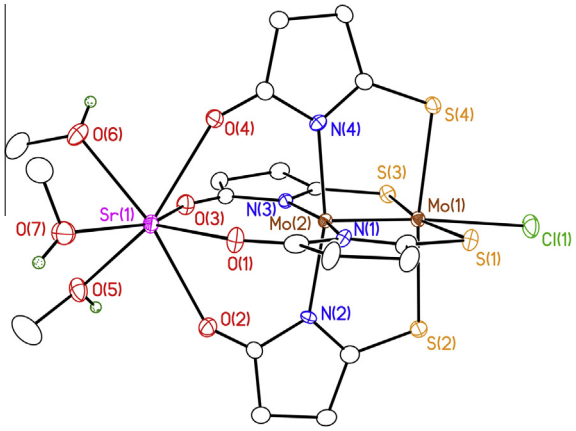

Fig. 3. X-ray crystal structure of the cation of **4**·2CH_3OH. All non-hydrogen atoms are drawn as 50% thermal probability ellipsoids. All hydrogen atoms except the alcohol hydrogens of methanols are omitted for clarity.

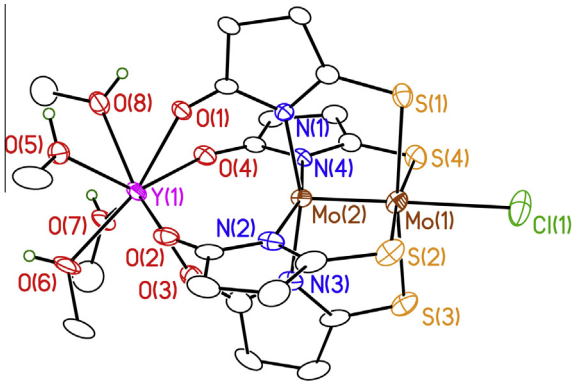

Fig. 4. X-ray crystal structure of the cation of **5**·1.6CH_3OH. All non-hydrogen atoms are drawn as 50% thermal probability ellipsoids. All hydrogen atoms, except those on the alcohol groups, and all disordered components are omitted for clarity.

bond distance is also shorter than those of **1**·py and **1-dim.** Another set of heterotrimetallic linear chain compounds recently reported by our group ($Mo_2Ru(dpa)_4Cl_2$, Mo_2–Cl = 2.5262(6) Å, and $[Mo_2Ru(dpa)_4Cl_2]OTf$, Mo_2–Cl = 2.4637(5) Å) have shorter Mo_2–Cl bond distances caused by covalent bonding between Ru and Mo_2 [5a,16]. The Mo_2–Cl bond distance of **3-dim**·5.5 MeCN is the shortest known for a M···Mo_2 heterotrimetallic compound in which M interacts with the Mo_2 unit in a purely Coulombic fashion. Unlike the MeOH solvent molecules of **3**·2MeOH, The MeCN solvent molecules of **3-dim**·5.5 MeCN are unable to form hydrogen bonds with the axial chlorides. Without the hydrogen bonding interaction competing with the $[Mo_2]^{4+}$ core for the axial Cl^-, structure **3-dim**·5.5 MeCN can support a shorter Mo–Cl bond distance.

Structure **5**·1.6MeOH contains an eight-coordinate Y^{3+} ion that is coordinated by the four SNO5 ligands and four MeOH ligands in a square anti-prismatic arrangement. Like **3**·2MeOH and **4**·2MeOH, **5**·1.6MeOH has a hydrogen bond between one of the partially occupied MeOH solvent molecules and the axial Cl^-. The axial Cl^- attached to the Mo_2 unit is compositionally disordered with a triflate anion (Cl^- component: 85.5(5)%). This compositional disorder is representative of the bulk sample as evidenced by the elemental analysis data (*vide supra*). This structure has a Y···Mo_2 distance of 3.745(2) Å, which is slightly longer than the Ca···Mo_2 distance in **3**·2MeOH as the Y^{3+} ion is repelled by the Mo^{2+} ions more strongly than Ca^{2+} is. The Mo_2–Cl bond distance is slightly shorter than that of **3**·2MeOH and **4**·2MeOH, an effect that can be attributed to the increased charge of Y^{3+} as compared with either Ca^{2+} or Sr^{2+}.

In general, the increased charge of the Lewis acidic cation influences the dimolybdenum center, making it more Lewis acidic and shortening the Mo_2–Cl bond distance. However, this effect is mitigated by the increased repulsion between the $[Mo_2]^{4+}$ moiety and the cation resulting from the cation's increased charge as well as by the formation of hydrogen bonds with solvent methanol.

3.3. Electrochemistry

Cyclic voltammograms (CV) of compounds $[LiMo_2(SNO5)_4][PF_6]$ (**1a**), $[NaMo_2(SNO5)_4][PF_6]$ (**2a**), $[CaMo_2(SNO5)_4][PF_6]_2$ (**3a**), and $[YMo_2(SNO5)_4][PF_6]_3$ (**5a**) were taken in propylene carbonate with 2 mM analyte and 100 mM NEt_4PF_6 as the electrolyte. Compounds **1a**, **2a**, **3a**, and **5a** were generated *in situ* by reacting **1**, **2**, **3**, and **5** with $TlPF_6$ in propylene carbonate in order to strip away the axial chloride. This was a necessary step for obtaining high quality CVs of the compounds because the $Mo_2^{4+/5+}$ redox waves of some compounds overlapped with the $Cl^-/Cl^\cdot$ redox waves. Solid TlCl was removed by filtration, and CVs were taken on the filtered solutions of **1a**, **2a**, **3a**, and **5a**. Each of these exhibits a quasi-reversible $Mo_2^{4+/5+}$ redox wave that moves to a higher potential as M^{n+} is added to the solution. These CVs are consistent with metal ion-coupled electron transfer [17], and they indicate that each of these compounds reversibly binds M^{n+}, as we previously reported for the electrochemistry of **1**. Further, these CVs are substantially different than those of the previously reported *trans*-2,2-$Mo_2(SNO5)_4$ and *cis*-2,2-$Mo_2(SNO5)_4$, ruling out the possibility that **1a**, **2a**, **3a**, and **5a** undergo ligand rearrangement upon halide abstraction. Thus, the conclusions we draw from this electrochemical study are based on the reasonable assumption that the solution structures of **1a**, **2a**, **3a**, and **5a**, are similar to those of their halogenated counterparts.

Each solution was titrated with a solution of $M(OTf)_n$ until the redox wave was no longer affected by additional aliquots of M $(OTf)_n$ solution. The final CVs for each compound are shown in Fig. 5 and the redox potentials as well as the amount M^{n+} added to solution are reported in Table 3. The charge of the Lewis acid, and thus the charge of the $[MMo_2(SNO5)_4]^{n+}$ cation, greatly

Table 2
Selected bond distances for compounds **1–5**.

Compound	Mo–Mo (Å)	M···Mo (Å)	Mo_2–Cl (Å)	M^{n+}–O_{SNO5} (Å)	M^{n+} ionic radius (Å)[a]	Refs.
1·py	2.1357(3)	3.075(5)	2.6533(6)	2.182[6]	0.90	[5c]
1-dim	2.1354(8)	3.049(6)	2.644(1)	2.185[7]	0.90	[5c]
2·4py	2.1377(7)	3.505(2)	2.776(1)	2.434(2)	1.14	This work
3·2MeOH	2.1306(6)	3.699(1)	2.7023(9)	2.4422[9]	1.20	This work
3-dim·5.5 MeCN	2.1361[8]	3.711[1]	2.630[1]	2.439[2]	1.20	This work
4·2MeOH	2.1333(5)	3.8138(5)	2.707(1)	2.554[2]	1.35	This work
5·1.6MeOH	2.120(1)	3.745(2)	2.699(3)	2.374[3]	1.16	This work

[a] Values taken from Ref. [18].

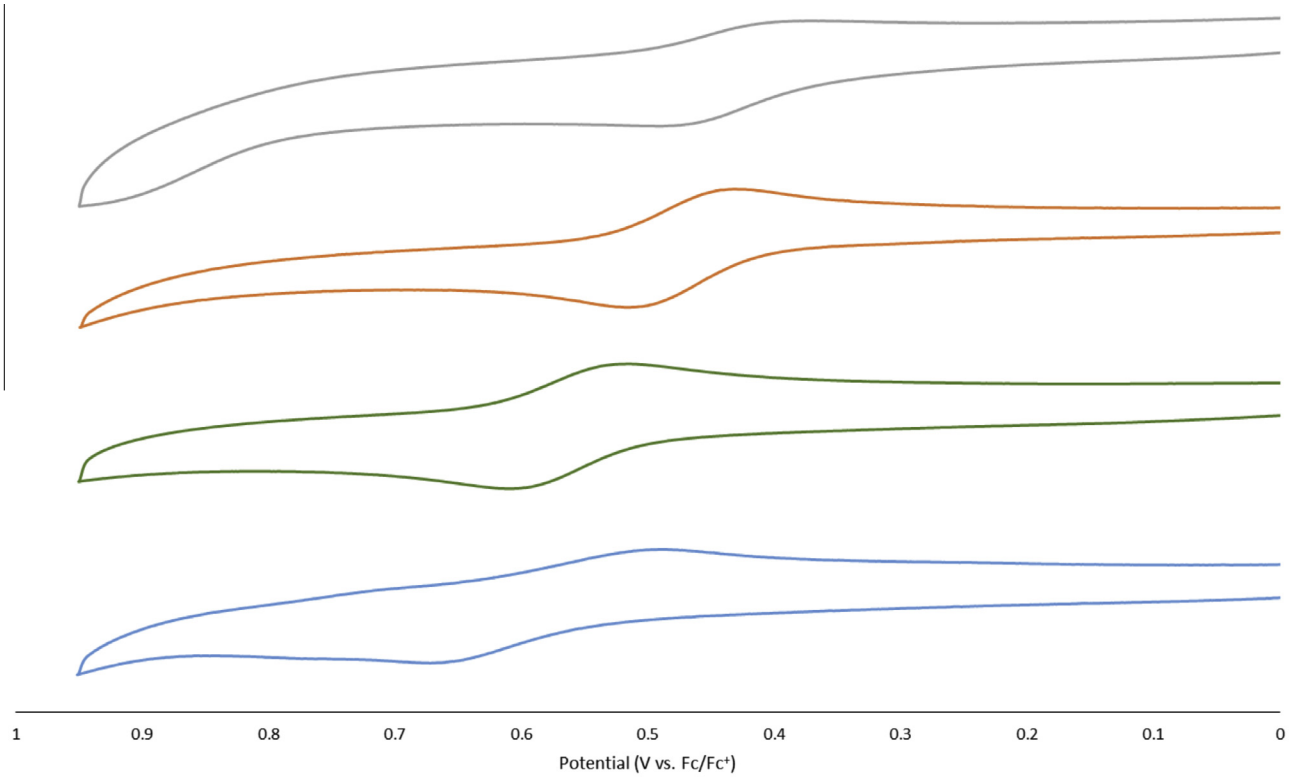

Fig. 5. Cyclic voltammograms of $[LiMo_2(SNO5)_4]^+$ (**1a**, gray) $[NaMo_2(SNO5)_4]^+$ (**2a**, orange), $[CaMo_2(SNO5)_4]^{2+}$ (**3a**, green), and $[YMo_2(SNO5)_4]^{3+}$ (**5a**, blue). The CVs were taken in PC with 2 mM analyte and 100 mM NEt_4PF_6. The currents are normalized. (Color online.)

Table 3
Electrochemical potentials of **1a**, **2a**, **3a**, and **5a**.

Compound	$E_{1/2}$ vs. F_c/F_c^+ (mV)	Equivalents M^{n+} added
1a	446	20
2a	480	19
3a	567	25
5a	579	8

influences the $Mo_2^{4+/5+}$ redox potential. The ionic radii of Na^+, Ca^{2+}, and Y^{3+} have a narrow range of 0.06 Å. Thus, the differences in the CVs of **2a**, **3a**, and **5a** are based primarily on the charge of M^{n+}, rather than differences in the ionic radius. As the charge of M^{n+} in these compounds increases from +1 to +3, this potential shifts from 480 mV to 579 mV. Given the ease of swapping one cation for another in these systems, these results demonstrate a simple method to reliably tune the redox potential of the $Mo_2^{4+/5+}$ couple over a range of 100 mV.

4. Conclusions

We describe here the synthesis of four new M···Mo_2 compounds in which M is a Group I, II, or III cation. Three of these compounds (**2**, **3**, and **5**) follow a diagonal trend and have very similar ionic radii, allowing the effect of cation charge on the Lewis acidity of $[Mo_2]^{4+}$ and $[Mo_2]^{4+/5+}$ redox couple to be probed. Compound **4** has the same cation charge as **3**, but it has a larger ionic radius, allowing the effect of increasing the M···Mo_2 distance on $[Mo_2]^{4+}$ Lewis acidity to be examined. Increasing the charge of the M^{n+} does increase the Lewis acidity of $[Mo_2]^{4+}$, shortening the Mo_2–Cl bond distance, however the effect is attenuated by an increase in the M···Mo_2 distance resulting from increased repulsion between M^{n+} and $[Mo_2]^{4+}$. Increasing the M···Mo_2 distance has a modest effect that decreases $[Mo_2]^{4+}$ Lewis acidity and slightly increases the Mo_2–Cl bond distance. The charge of M^{n+} has a profound impact on the redox potential of the $[Mo_2]^{4+/5+}$ couple. Increasing the charge of M^{n+} from $n = 1$ to $n = 3$ allows the $[Mo_2]^{4+/5+}$ redox couple to be tuned over a 100 mV range.

Acknowledgements

The authors thank Tristan R. Brown for his help in obtaining elemental analysis data on these compounds. Financial support was provided under NSF Grant CHE-1300464 and a generous gift from Paul J. Bender (X-ray diffraction and NMR spectroscopy instrumentation). Finally, the authors wish Malcolm Chisholm a very happy birthday.

Appendix A. Supplementary data

CCDC 1413783-1413787 contains the supplementary crystallographic data for **2**·4py, **3**·2MeOH, **3-dim**·5.5MeCN, **4**·2MeOH, **5**·1.6MeOH. These data can be obtained free of charge via http://www.ccdc.cam.ac.uk/conts/retrieving.html, or from the Cambridge Crystallographic Data Centre, 12 Union Road, Cambridge CB2 1EZ, UK; fax: (+44) 1223-336-033; or e-mail: deposit@ccdc.cam.ac.uk.

Supplementary data associated with this article can be found, in the online version, at http://dx.doi.org/10.1016/j.poly.2015.09.028.

References

[1] (a) F.A. Cotton, C.A. Murillo, R.A. Walton, Multiple Bonds Between Metal Atoms, 3rd ed., Springer Science and Business Media Inc., New York, 2005;
(b) L.R. Falvello, B.M. Foxman, C.A. Murillo, Inorg. Chem. 53 (2014) 9441.
[2] (a) G. Li Manni, A.L. Dzubak, A. Mulla, D.W. Brogden, J.F. Berry, L. Gagliardi, Chem. Eur. J. 18 (2012) 1737;
(b) B.S. Dolinar, J.F. Berry, Dalton Trans. 43 (2014) 6165;
(c) J. Hicks, S.P. Ring, N.J. Patmore, Dalton Trans. 41 (2012) 6641;
(d) M.H. Chisholm, N.J. Patmore, Acc. Chem. Res. 40 (2007) 19;
(e) L.A. Wilkinson, L. McNeill, A.J. Meijer, N.J. Patmore, J. Am. Chem. Soc. 135

(2013) 1723;
(f) L.A. Wilkinson, L. McNeill, P.A. Scattergood, N.J. Patmore, Inorg. Chem. 52 (2013) 9683;
(g) B.G. Alberding, S.E. Brown-Xu, M.H. Chisholm, T.L. Gustafson, C.R. Reed, V. Naseri, Dalton Trans. 41 (2012) 13097;
(h) M.H. Chisholm, T.L. Gustafson, C. Turro, Acc. Chem. Res. 46 (2013) 529;
(i) B.G. Alberding, M.H. Chisholm, C.B. Durr, J.C. Gallucci, Y. Ghosh, T.F. Spilker, Dalton Trans. 43 (2014) 11397;
(j) B.G. Alberding, M.H. Chisholm, Y.-H. Chou, J.C. Gallucci, Y. Ghosh, T.L. Gustafson, N.J. Patmore, C.R. Reed, C. Turro, Inorg. Chem. 48 (2009) 4394;
(k) B.G. Alberding, M.H. Chisholm, Y.H. Chou, Y. Ghosh, T.L. Gustafson, Y. Liu, C. Turro, Inorg. Chem. 48 (2009) 11187;
(l) B.G. Alberding, M.H. Chisholm, J.A. Gallucci, Y. Ghosh, T.L. Gustafson, Proc. Natl. Acad. Sci. U.S.A. 108 (2011) 8152;
(m) B.G. Alberding, M.H. Chisholm, T.L. Gustafson, C.R. Reed, N. Singh, C. Turro, J. Cluster Sci. 20 (2009) 307;
(n) B.G. Alberding, M.H. Chisholm, B.J. Lear, V. Naseri, C.R. Reed, Dalton Trans. 40 (2011) 10658;
(o) M.H. Chisholm, J.S. D'Acchioli, B.D. Pate, N.J. Patmore, Inorg. Chem. 44 (2005) 1061.

[3] C.A. Murillo, Aust. J. Chem. 67 (2014) 972.

[4] (a) M. Nippe, E. Victor, J.F. Berry, Inorg. Chem. 48 (2009) 11889;
(b) D.W. Brogden, Y. Turov, M. Nippe, G. Li Manni, E.A. Hillard, R. Clérac, L. Gagliardi, J.F. Berry, Inorg. Chem. 53 (2014) 4777.

[5] (a) D.W. Brogden, J.F. Berry, Inorg. Chem. 53 (2014) 11354;
(b) D.W. Brogden, J.H. Christian, N.S. Dalal, J.F. Berry, Inorg. Chim. Acta 424 (2015) 241;
(c) B.S. Dolinar, J.F. Berry, Inorg. Chem. 52 (2013) 4658;
(d) M. Nippe, J.F. Berry, J. Am. Chem. Soc. 129 (2007) 12684;
(e) M. Nippe, E. Bill, J.F. Berry, Inorg. Chem. 50 (2011) 7650;
(f) M. Nippe, Y. Turov, J.F. Berry, Inorg. Chem. 50 (2011) 10592;
(g) M. Nippe, E. Victor, J.F. Berry, Eur. J. Inorg. Chem. 2008 (2008) 5569;
(h) M. Nippe, J. Wang, E. Bill, H. Hope, N.S. Dalal, J.F. Berry, J. Am. Chem. Soc. 132 (2010) 14261;
(i) K. Mashima, Y. Shimoyama, Y. Kusumi, A. Fukumoto, T. Yamagata, M. Ohashi, Eur. J. Inorg. Chem. 2007 (2007) 235;
(j) M. Ohashi, A. Shima, T. Rüffer, H. Mizomoto, Y. Kaneda, K. Mashima, Inorg. Chem. 46 (2007) 6702;
(k) K. Pal, K. Nakao, K. Mashima, Eur. J. Inorg. Chem. 2010 (2010) 5668;
(l) M.H. Chisholm, A.M. Macintosh, Chem. Rev. 105 (2005) 2949;
(m) B. Li, H. Zhang, L. Huynh, M. Shatruk, E.V. Dikarev, Inorg. Chem. 46 (2007) 9155;
(n) M. Koeberl, M. Cokoja, W.A. Herrmann, F.E. Kuehn, Dalton Trans. 40 (2011) 6834.

[6] (a) K. Jansen, K. Dehnicke, D. Fenske, Z. Naturforsch., B 40 (1985) 13;
(b) F. Apfelbaum, A. Bino, Inorg. Chim. Acta 155 (1989) 191;
(c) F.A. Cotton, L.R. Falvello, A.H. Reid Jr., W.J. Roth, Acta Crystallogr. C 46 (1990) 1815;
(d) B. Udovic, I. Leban, P. Šegedin, Croat. Chem. Acta 72 (1999) 477.

[7] (a) J.V. Brencic, F.A. Cotton, Inorg. Chem. 8 (1969) 7;
(b) J.V. Brencic, F.A. Cotton, Inorg. Chem. 8 (1969) 2698;
(c) I. Leban, P. Šegedin, Inorg. Chim. Acta 85 (1984) 181;
(d) F.A. Cotton, J.H. Matonic, D.de O. Silva, Inorg. Chim. Acta 234 (1995) 115.

[8] (a) F.G. Adly, A. Ghanem, Chirality 26 (2014) 692;
(b) J. Hansen, H.M.L. Davies, Coord. Chem. Rev. 252 (2008) 545;
(c) A.F. Trindade, J.A.S. Coelho, C.A.M. Afonso, L.F. Veiros, P.M.P. Gois, ACS Catal. 2 (2012) 370;
(d) K.P. Kornecki, J.F. Berry, D.C. Powers, T. Ritter, Metal-Metal Bond-Containing Complexes as Catalysts for C-H Functionalization, in: K.D. Karlin (Ed.) Prog. Inorg. Chem., John Wiley & Sons, Inc., Hoboken, 2014, pp. 225–302.;
(e) K.P. Kornecki, J.F. Berry, Chem. Eur. J. 17 (2011) 5827;
(f) K.P. Kornecki, J.F. Berry, Eur. J. Inorg. Chem. (2012) 562;
(g) K.P. Kornecki, J.F. Berry, Chem. Commun. 48 (2012) 12097.

[9] K.P. Kornecki, J.F. Briones, V. Boyarskikh, F. Fullilove, J. Autschbach, K.E. Schrote, K.M. Lancaster, H.M.L. Davies, J.F. Berry, Science 342 (2013) 351.

[10] (a) E.Y. Tsui, R. Tran, J. Yano, T. Agapie, Nature Chem. 5 (2013) 293;
(b) Y.J. Park, J.W. Ziller, A.S. Borovik, J. Am. Chem. Soc. 133 (2011) 9258;
(c) I.S. Ke, J.S. Jones, F.P. Gabbai, Angew. Chem., Int. Ed. Engl. 53 (2014) 2633;
(d) T.P. Lin, F.P. Gabbaï, J. Am. Chem. Soc. 134 (2012) 12230;
(e) H. Yang, F.P. Gabbaï, J. Am. Chem. Soc. 136 (2014) 10866.

[11] U. Berg, J. Sandström, Acta Chem. Scand. 20 (1966) 689.

[12] G. Holste, H. Schäfer, Z. Anorg. Allg. Chem. 391 (1972) 263.

[13] (a) Bruker-AXS, in, Bruker AXS, Madison, WI, 2014.;
(b) L. Kraus, R. Herbst-Irmer, G.M. Sheldrick, D. Stalke, J. Appl. Crystallogr. 48 (2015) 3.

[14] (a) G.M. Sheldrick, XS, Georg-August-Universität Göttingen, Göttingen, Germany, 2013;
(b) G.M. Sheldrick, Acta Crystallogr. C 71 (2015) 3;
(c) O.V. Dolomanov, L.J. Bourhis, R.J. Gildea, J.A.K. Howard, H. Puschmann, J. Appl. Crystallogr. 42 (2009) 339.

[15] F.H. Allen, Acta Crystallogr. B 58 (2002) 380.

[16] D.W. Brogden, J.F. Berry, Inorg. Chem. 54 (2015) 7660.

[17] (a) S. Fukuzumi, K. Ohkubo, Coord. Chem. Rev. 254 (2010) 372;
(b) S. Fukuzumi, K. Ohkubo, Y. Morimoto, Phys. Chem. Chem. Phys. 14 (2012) 8472.

[18] R.D. Shannon, Acta Crystallogr. A 32 (1976) 751.